Dalton
Transactions

RSCPublishing

PAPER

View Article Online
View Journal | View Issue

Cite this: *Dalton Trans.*, 2013, **42**, 13151

Synthesis and characterization of Co(III) amidoamine complexes: influence of substituents of the ligand on catalytic cyclic carbonate synthesis from epoxide and carbon dioxide†

Punnamchandar Ramidi,[a] Nikolay Gerasimchuk,[b] Yashraj Gartia,[a]
Charlette M. Felton[a] and Anindya Ghosh*[a]

Received 23rd May 2013,
Accepted 6th July 2013

DOI: 10.1039/c3dt51352a

www.rsc.org/dalton

A series of amidoamine ligands (**1**) and their cobalt(III) complexes (**2**) were synthesized and characterized by various spectroscopic techniques including ^{1}H-NMR and X-ray crystallographic techniques. X-ray crystallography shows that one of the complexes, **2a**, forms a chiral coordination polymer due to bridge formation with Li^+ associated with the complex, although the ligand is achiral. Complex **2** was employed for catalytic synthesis of cyclic carbonates from epoxides and carbon dioxide (CO_2) in a solvent free condition. A strong influence of the substituents on the ligand **1** was revealed by the varied activity of complex **2**. The presence of electron withdrawing groups such as chloro (**2b**) and nitro (**2c**) increases the Lewis acidity of the catalyst, which, in turn, enhances the catalytic activity of **2**. An electron withdrawing group containing complexes (**2b** and **2c**) showed exceptionally high catalytic activity with a turnover frequency (TOF) of 662 and 602 h^{-1} respectively at 130 °C and 300 psig CO_2 pressure. On the other hand, our studies indicate that a catalyst with an electron releasing group (**2d**) showed relatively lower activity with a TOF of 488 h^{-1} under similar reaction conditions. Our results show that cobalt(III) complexes follow the reactivity order of **2d** < **2a** < **2c** < **2b**.

1. Introduction

Commercial production of many useful chemicals and polymers has been heavily dependent on petroleum feedstock. Since crude oil is a non-renewable resource, its depletion is a cause of serious concern. Many efforts have been made over the past few decades to develop alternative and sustainable materials as a solution to this problem.[1–7] In terms of green chemistry and sustainable development, the use of renewable resources, such as carbon dioxide (CO_2), as a starting material for the production of industrially important organic compounds has been a topic of interest to the scientific community.[6–8] One such utilization of CO_2 is the synthesis of cyclic carbonates *via* cycloaddition of CO_2 to epoxide (Scheme 1). Cyclic carbonates are colorless, odorless, and biodegradable chemicals with low toxicity.[9–11] Because of these advantages, cyclic carbonates have found use in several applications which includes as solvents and precursors for synthesizing various pharmaceutically and industrially important chemicals and polymers.[12–20]

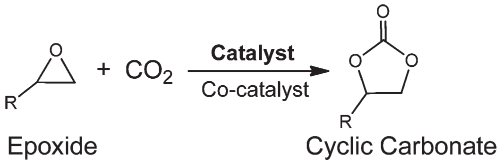

Scheme 1 Synthesis of cyclic carbonate using CO_2 and epoxide.

In the past few decades, several homogeneous and heterogeneous catalytic systems such as ionic liquids,[21,22] supported metal oxides,[23,24] alkali metal salts,[25] quaternary ammonium salts,[26] and transition metal complexes,[27–35] have been employed in cyclic carbonate synthesis. However, attention has been paid to the development of catalysts with a high efficiency and that work under mild reaction conditions.

---

[a] *Department of Chemistry, University of Arkansas at Little Rock, 2801 South University Avenue, Little Rock, AR 72204, USA. E-mail: axghosh@ualr.edu; Fax: +1 501 569 8838; Tel: +1 501 569 8827*

[b] *Department of Chemistry, Temple Hall 456, Missouri State University, Springfield, Missouri 65897, USA*

† Electronic supplementary information (ESI) available: Synthetic procedure and characterization details of all ligands and cobalt complexes including X-ray crystallographic information and data for **2a**, **2b** together with PLATON check-CIF reports, product characterizations, and Hammett plot are given in ESI. CCDC 936734 and 936336. For ESI and crystallographic data in CIF or other electronic format see DOI: 10.1039/c3dt51352a

Among them, bimetallic and one component binary catalytic systems were prominent in this pursuit.[34–38]

For the cycloaddition of CO_2 to epoxide, activation of epoxide and subsequent epoxide ring opening are vital steps. Generally, such a cycloaddition reaction requires a Lewis acidic catalyst and a Lewis base as a co-catalyst.[29,39] Lewis acidity of any catalyst for such a reaction should play an important role. It is evident from previous reports that the increase in Lewis acidity of the metal complexes enhances their catalytic activity. For example, metal-based catalysts with high oxidation numbers are more efficient in cycloaddition reactions.[21,39–41] In the literature many reactive catalysts are made of Al(III) and Zn(II), which are fairly strong Lewis acids.[41] Previously, we also reported the influence of Lewis acids on catalytic activity. In our study we showed that when we replaced counter cation Li^+ of the Cr(V) amido macrocyclic complex with Na^+ and K^+, the catalytic activity dropped dramatically.[28] We rationalized the observation based on the fact that Li^+ is more Lewis acidic and, hence, accounts for more activity compared to less Lewis acidic counter cations (Na^+ and K^+) of the Cr(V) complex. We also studied the activity of various alkali halides with Lewis bases for the cycloaddition of CO_2 to epoxides and increased activity was observed with increasing Lewis acidity of the alkali halides.[27,28] Apart from these findings, we recently reported the synthesis of cyclic carbonates and oxazolidinones using a series of chlorostannoxane catalysts.[42–44] The catalysts showed a strong dependence on its substituents. The catalyst with high Lewis acidity, as dictated by the substituents on the Sn centers of chlorostannoxanes, furnishes high reactivity towards both cyclic carbonate and oxazolidinone synthesis.

Focusing on the possibility of increasing the electrophilicity of the metal complexes by introducing electron withdrawing groups, we developed a series of Co(III) metal complexes (**2**) of various amidoamine ligands (**1**) bearing various electron withdrawing and electron donating groups on the aromatic ring of the ligands (Fig. 1). Co(III) complexes (**2**) of corresponding ligands (**1**) were successfully characterized by using various analytical techniques. X-ray crystallographic studies of complex **2a** reveal that it is an anionic cobalt complex with two axial halides and a Li^+ counter cation. Interestingly, the complex crystallizes in a chiral space group due to the formation of coordination polymers, even though the ligand is not chiral. Crystals of complex **2b** were observed as a neutral complex with an axial halide ligand. Catalytic activities of **2a–2d** were studied on cycloaddition of CO_2 to epoxide in the presence of 4-dimethylaminopyridine (DMAP) as a co-catalyst. Based on the variation in their electron withdrawing (**2b** and **2c**) and electron donating (**2a** and **2d**) properties, we have observed that dichloro substituted Co(III) amidoamine complex (**2b**) produced the high catalytic activity with a TOF of 662 h^{-1} on propylene carbonate production. On the other hand, complex **2d**, which contains electron releasing methyl groups, showed low catalytic activity (TOF 488 h^{-1}). A linear relationship was obtained when TOF (h^{-1}) of different catalysts were plotted against the Hammett parameters (σ_m) of various substituents corroborating our hypothesis on reactivity and the effect of electron withdrawing and releasing groups on Lewis acidity. In order to understand the activity of these cobalt complexes, optimization studies were performed using propylene oxide as the reference substrate.

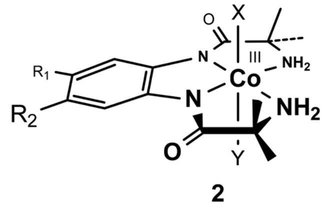

2

	-R1	-R2	X
2a	-H	-H	Br
2b	-Cl	-Cl	Br
2c	-H	$-NO_2$	Br
2d	$-CH_3$	$-CH_3$	Br

X= Y = Cl or Br*
or
X= Cl or Br, Y= Solvent

Fig. 1 Structure of the catalysts (R_1, R_2 are different electron donating and electron withdrawing groups on the catalyst structure). *Counter cation is Li^+.

2. Results and discussion

2.1. Synthesis, characterization and structural studies of cobalt complexes

Co(III) complexes (Fig. 1) of the corresponding amidoamine ligands were synthesized by taking the ligand in tetrahydrofuran (THF) under an inert atmosphere. Using *n*-butyllithium as a strong base, the ligand was deprotonated and reacted with anhydrous Co(II) chloride. Finally, the desired Co(III) complex was obtained under air exposure. The resulting Co complex was found to be highly stable in air and moisture. All these Co(III) complexes (**2a–2d**) were characterized by performing FT-IR, ESI-MS, NMR, and elemental analysis studies.

For structure elucidation of these complexes, Co(III) complexes were synthesized by using cobalt(II) halide as a metal precursor. Characterization details of complexes **2a–2d** are explained here. Elemental analysis values for complexes **2a–2d** matched well with the theoretical values (see the Experimental section). The strong and sharp NMR signals (Fig. 2) of the complexes indicate that all the complexes are low spin d^6 systems. The aromatic proton peaks of the complexes are shifted to lower field compared with relevant ligands. Protons of methyl groups ($-CH_3$) attached to the amino acid part of the ligand show a characteristic singlet peak in the region of δ = 1.6–1.5 ppm. On the other hand, CH_3 protons attached to an aromatic ring in **2d** show a characteristic singlet peak at δ = 2.06 ppm. One extra peak was observed at δ = 2.06 ppm (Fig. 2) for **2b** and **2d**. This extra peak was assigned to an acetonitrile molecule which was used for crystallization and further confirmed by X-ray crystallography study. The Fourier transform infrared spectroscopic (FT-IR) analysis of the complexes showed the characteristic carbonyl stretching frequencies in the range of 1580–1600 cm^{-1}, and NH stretching 3220–3460 cm^{-1}. A characteristic C–Cl stretching frequency at 678 cm^{-1} for **2b** and a NO_2 stretching frequency at 1308 cm^{-1}

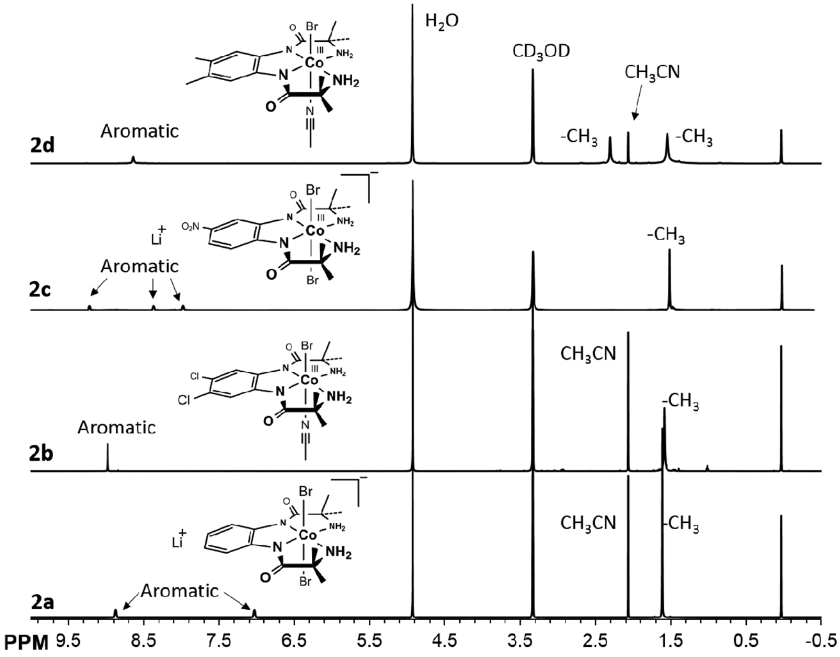

Fig. 2 ^{1}H NMR spectra of **2a**, **2b**, **2c** and **2d**.

for **2c** were observed. Complexes **2a**–**2d** were further characterized by using ESI-MS (Fig. S9, ESI†). X-ray quality crystals of complexes **2a** and **2b** with bromide were obtained from slow evaporation of solvent acetonitrile in which the catalyst was dissolved previously. X-ray crystallographic studies were performed on suitable **2a** and **2b** crystals.

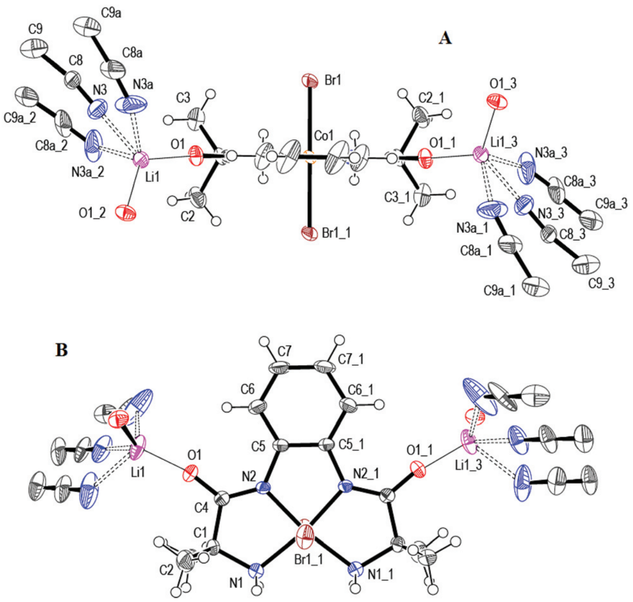

Fig. 3 Two orthogonal views of the **2a** complex structure: A – side view, B – top view showing the numbering scheme; an ORTEP drawing at the 50% thermal ellipsoids probability level. Symmetry transformations: #1 *x*, *y*, *z*; #2 −*x*, −*y*, *z* + 1/2, #3 −*x*, *y*, −*z* + 1/2; #4 *x*, −*y*, −*z*; #5 *x* + 1/2, *y* + 1/2, *z*; #6 −*x* + 1/2, −*y* + 1/2, *z* + 1/2; #7 −*x* + 1/2, *y* + 1/2, −*z* + 1/2; #8 *x* + 1/2, −*y* + 1/2, −*z*.

Molecular structure and numbering scheme for complex **2a** are shown in Fig. 3, while selected bond distances and valence angles are summarized in Table 2. This compound represents the cationic complex of $Li(CoLBr_2)\cdot nCH_3CN$ composition and contains several disordered solvent molecules. It appears that disordered solvent molecules are clustered around a Li^+ cation from one side of the molecule (Fig. S12, ESI†), and are electrostatically attracted to the NH_2 groups of the amidoamine ligand (Fig. S13, ESI†). In addition to disorder, there was also their partial occupancy in the crystal lattice, which further complicated the structure determination. We refrained from using the PLATON SQUEEZ program in order not to alter experimental data which would affect chemical meaning in the structure. Although we were able to model non-hydrogen atoms in a disordered solvent, we were not able to locate H-atoms of the methyl groups on the difference map. Moreover, an attempt to place hydrogen atoms geometrically led to unstable refinement. Therefore, they were not included in final refinement cycles. Their absence did not affect overall quality of the structure due to the presence of 3 heavy atoms (Co, 2Br) in the structure. The Co(III) center in the complex is in a distorted octahedral environment comprised of two axial Br^- anions and 4 nitrogen atoms in the equatorial plane (Fig. 3). The bond distances of Co to aromatic N (deprotonated amide nitrogens) atoms and amine N (aliphatic amine nitrogens) atoms in **2a** are 1.862 Å and 1.958 Å, respectively. The $Co–N_{amide}$ distances are significantly shorter than the $Co–N_{amine}$ distances. Two axial bromine atoms are at equal distance from the Co metal center with 2.428 Å. Notable deviations in the four Co–N angles are observed, N(2)#1–Co–N(2), N(2)#1–Co(1)–N(1)#1, N(2)–Co(1)–N(1) angles with 86.2°, 85.11° and 85.11°, respectively, whereas N(1)–Co–N(1)#1 with a wider angle of 103.6°, which are found to be comparable with the earlier reported Co(III) complexes of 1,2-bis(2-pyridinecarboxamide)benzene ligand.[45,46]

Details of the geometry of the coordination polyhedron of the central atom are shown in Fig. S14 (ESI†). The presence of solvated with disordered CH_3CN molecules in Li^+ cations adds some peculiarity to the crystal structure of **2a**. Thus, the Li^+ counter cation acts as a bridge between anionic $[CoL(Br)_2]^-$ units (Fig. 3, L stands for a ligand). Li^+, being small in size, coordinates to relatively electron rich carbonyl groups of deprotonated amide bonds of the ligand to form a coordination polymer. The shape and configuration of the coordination polymer formed became chiral, although the Co(III) complex is, obviously, non-chiral. The result is crystallization of **2a** in a chiral space group *P*222(1) (#20) (Table 1), and because there are three heavy atoms present in the structure, their anomalous dispersion allowed reliable determination of the absolute configuration of the complex, which is reflected in its very low Flack parameter. Both Co(III) and Li^+ atoms occupy special positions in the unit cell.

Such chiral coordination polymers can be obtained by using chiral species and chiral additives, and by crystallization of achiral moieties without using any chiral additives, resulting in spontaneous chiral resolution, which is rare.[47–52] The use of chiral coordination polymers has been of growing scientific interest in recent years due to their potential applications in asymmetric catalysis, non-linear optics, and chiral separation.[47–49] Herein, we observed that complex **2a** crystallizes in a chiral space group *P*222(1) (#20), forming a coordination polymer. The metal center in **2a** forms six coordinated species with four nitrogen atoms (equatorial) and two bromide ions (axial), and it induces the chirality through the solvated Li^+ ions, which is intimately associated with the anionic units of the complex and forms bridges between them, resulting in a chiral coordination polymer with achiral units. We are currently investigating crystals of **2a** for further applications, especially in the field of asymmetric synthesis.

Fig. 4 shows the ORTEP diagram and the numbering scheme for complex **2b**. Details of the data collection and refinement parameters of complex **2b** are listed in Table 1, while selected bond lengths and valence angles are presented in Table 2. X-ray crystallographic studies demonstrate that the Co(III) complex crystallizes in the orthorhombic system in *Pnma* space group. The metal center is in a six coordinate octahedral environment comprised of four N atoms of the ligand moiety in the equatorial plane (two amine ligands and two deprotonated amide bonds) and two axial positions occupied with one bromide and one solvent molecule (acetonitrile). The bond distances of Co to aromatic N (deprotonated amide bond) atoms and amine N atoms in **2b** are 1.868 and 1.969 Å, respectively, which are similar to the previously reported Co(III) complexes of salen and macrocyclic ligands.[27,53] The distances between the metal center and axial atoms are 2.369 and 1.937 Å for Co–Br and Co–N ($NCCH_3$), respectively. The N–Co–N

Table 1 Crystal data and structure refinement for the studied Co(III) complexes

	2a	**2b**
Empirical formula	$C_{9.45}H_{10}BrCo_{0.50}Li_{0.50}N_{3.24}O$	$C_{16}H_{21}BrCl_2CoN_5O_2$
Formula weight	297.71	525.12
Temperature (K)	120(2)	120(2)
Wavelength	0.71073 Å	0.71073 Å
Crystal system	Orthorhombic	Orthorhombic
Space group	*P*222(1), #20	*Pnma*, #62
Unit cell dimensions (Å; °)	$a = 9.0155(12)$	$a = 10.2678(6)$
	$b = 17.429(2)$	$b = 13.4525(8)$
	$c = 15.794(2)$	$c = 14.9665(9)$ Å
	$\alpha = 90$	$\alpha = 90$
	$\beta = 90$	$\beta = 90$
	$\gamma = 90$	$\gamma = 90$
Volume ($Å^3$), *Z*	2481.8(6) $Å^3$, 8	2067.3(2), 4
Density (calculated)	1.594 Mg m^{-3}	1.687 Mg m^{-3}
Absorption coefficient (mm^{-1})	3.938	3.043
F(000)	1179	1056
Crystal size (mm)	0.25 × 0.13 × 0.10	0.49 × 0.27 × 0.22
Θ Range for data collection	2.54 to 27.16°	2.04 to 29.13°
Index ranges	$-11 \le h \le 11$	$-14 \le h \le 13$
	$-22 \le k \le 22$	$-18 \le k \le 18$
	$-20 \le l \le 20$	$-20 \le l \le 20$
Reflections collected	14 362	26 557
Independent reflections	2756 [R(int) = 0.0664]	2880 [R(int) = 0.0301]
Completeness to Θ	99.7%	99.6%
Absorption correction	Semi-empirical	Numerical
T(max) and *T*(min)	0.7455 and 0.5770	0.7620 and 0.5285
Refinement method	Full-matrix least-squares on F^2	
Data/restraints/parameters	2880/0/173	
Goodness-of-fit on F^2	0.989	1.091
Final *R* indices [$I > 2\sigma(I)$]	$R_1 = 0.0394$, $wR_2 = 0.0815$	$R_1 = 0.0383$, $wR_2 = 0.0941$
R indices (all data)	$R_1 = 0.0654$, $wR_2 = 0.0911$	$R_1 = 0.0466$, $wR_2 = 0.0987$
Largest peak and hole (e $Å^{-3}$)	0.469 and −0.548	0.922 and −1.106

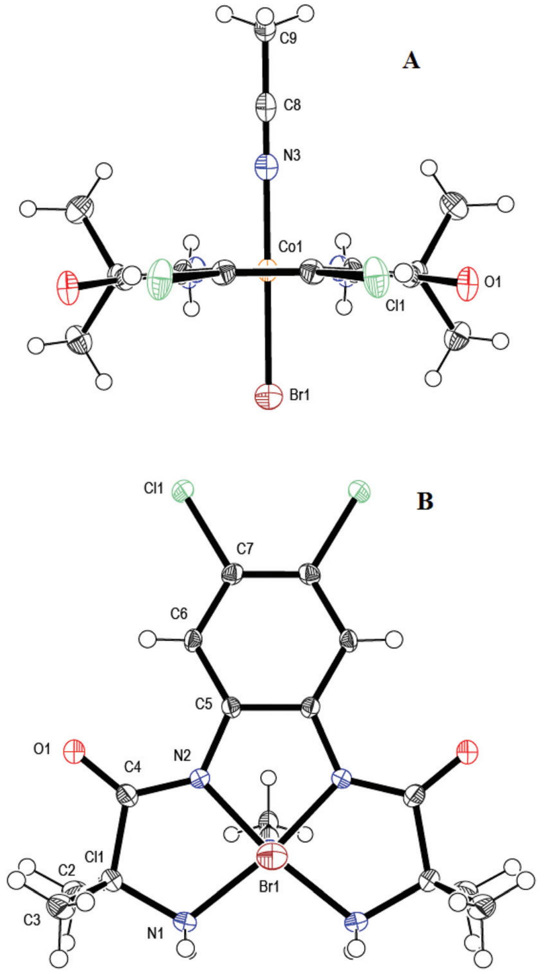

Fig. 4 Two orthogonal views of the **2b** complex structure: A – side view, B – top view showing the numbering scheme. Symmetry codes are: #1 *x*, *y*, *z*; #2 −*x*, −*y*, *z* + 1/2, #3 −*x*, *y*, −*z* + 1/2; #4 *x*, −*y*, −*z*; #5 *x* + 1/2, *y* + 1/2, *z*; #6 −*x* + 1/2, −*y* + 1/2, *z* + 1/2; #7 −*x* + 1/2, *y* + 1/2, −*z* + 1/2; #8 *x* + 1/2, −*y* + 1/2, −*z*.

Table 2 Selected bond length and valence angles in structures of Co(III) complexes

2a

Bonds (Å)		Angles (°)	
Ligand			
N(1)–C(1)	1.514(6)	N(1)–C(1)–C(4)	108.5(4)
C(1)–C(4)	1.533(7)	O(1)–C(4)–N(2)	126.5(4)
C(4)–N(2)	1.316(6)	N(2)–C(4)–C(1)	115.2(4)
N(2)–C(5)	1.419(6)	C(4)–O(1)–Li(1)	166.6(3)
C(4)–O(1)	1.253(5)	C(4)–N(2)–C(5)	127.5(4)
O(1)–Li(1)	1.810(8)	C(5)#1–C(5)–N(2)	113.6(3)
Metal center			
Co(1)–N(2)#1	1.862(4)	N(2)#1–Co(1)–N(2)	86.2(2)
Co(1)–N(2)	1.862(4)	N(2)#1–Co(1)–N(1)	171.29(18)
Co(1)–N(1)	1.958(4)	N(2)–Co(1)–N(1)	85.11(17)
Co(1)–N(1)#1	1.958(4)	N(1)–Co(1)–N(1)#1	103.6(2)
Co(1)–Br(1)#1	2.4279(5)	N(2)#1–Co(1)–Br(1)#1	91.09(5)
Co(1)–Br(1)	2.4279(5)	N(2)–Co(1)–Br(1)#1	91.53(5)
		N(1)#1–Co(1)–Br(1)#1	88.47(13)
		N(1)#1–Co(1)–Br(1)	89.31(13)
		Br(1)#1–Co(1)–Br(1)	176.42(5)

Symmetry transformations used to generate equivalent atoms: #1 −*x*, *y*, −*z* − 1/2

2b

Bonds (Å)		Angles (°)	
Ligand			
C(1)–N(1)	1.509(4)	N(1)–C(1)–C(4)	109.6(2)
C(1)–C(4)	1.551(4)	O(1)–C(4)–N(2)	127.0(2)
C(4)–O(1)	1.233(3)	O(1)–C(4)–C(1)	119.8(2)
C(4)–N(2)	1.342(3)	N(2)–C(4)–C(1)	113.2(2)
C(5)–N(2)	1.403(3)	C(4)–N(2)–C(5)	127.0(2)
C(7)–Cl(1)	1.735(3)	C(7)#1–C(7)–Cl(1)	121.03(9)
		C(6)–C(7)–Cl(1)	118.26(19)
Metal center			
Br(1)–Co(1)	2.3690(7)	N(2)–Co(1)–N(2)#1	86.58(13)
Co(1)–N(2)	1.868(2)	N(2)#1–Co(1)–N(3)	89.70(10)
Co(1)–N(2)#1	1.868(2)	N(2)#1–Co(1)–N(1)#1	85.19(10)
Co(1)–N(3)	1.937(4)	N(3)–Co(1)–N(1)#1	91.77(10)
Co(1)–N(1)#1	1.969(2)	N(2)#1–Co(1)–N(1)	171.63(10)
Co(1)–N(1)	1.969(2)	N(1)#1–Co(1)–N(1)	102.99(14)
		N(2)#1–Co(1)–Br(1)	90.13(7)
		N(3)–Co(1)–Br(1)	179.77(10)
		N(1)–Co(1)–Br(1)	88.37(8)

Symmetry transformations used to generate equivalent atoms: #1 *x*, −*y* + 1/2, *z*

bond angle between cobalt and aromatic N atoms is 86.58° and the N–Co–N bond angle between Co and two amine N atoms is 102.99°. Details of the geometry of the Co(III) coordination polyhedron in complex **2b** can be found in Fig. S14 (ESI†). Complete details of the X-ray crystallography studies are given in the ESI.† Unlike **2a**, neither **2b** forms any coordination polymer nor does it crystallize into a chiral space group. Complex **2b** is a neutral compound and as a result it does not have any Li cation, which is essential to interconnect different cobalt units by coordinating to amide oxygen atoms and solvents to yield a chiral material.

2.2 Optimization of reaction parameters

Due to the solubility of the participating components in the epoxide substrates, no co-solvent was used. Under the applied reaction conditions, *i.e.* 130 °C, 300 psig CO_2 pressure in 3 h, little or no product was observed without the use of either catalyst or co-catalyst, indicating that the reaction needs an active catalytic system. Based on our previous reports on propylene carbonate production,[27,28] the addition of Lewis base as a co-catalyst has shown a strong effect on the catalytic activity. The reaction products were confirmed by the presence of the respective molecular ion peaks in GC/MS analysis and a broad infrared peak at ν 1800 cm^{-1}. The absence of any other carbonate peaks in the IR spectra indicates high product selectivity. Gas chromatography of the reaction mixture shows the presence of the product as the sole component besides unreacted epoxide, suggesting high reaction selectivity. ^1H- and ^{13}C-NMR spectra were also used in certain cases to characterize the products (see ESI†).

Table 3 summarizes the activity of cobalt complexes (**2a–2d**) on cycloaddition of CO_2 with propylene oxide under solvent free conditions. Initially, we studied the activity of cobalt complexes on cycloaddition of CO_2 to propylene oxide in the

Table 3 Study of various co-catalysts on the reaction TOF for the catalyst **2**/co-catalysts system

Entry	2/co-catalyst	TOF[a] (h^{-1})
1	**2a** only	38
2	**2b** only	64
3	**2c** only	52
4	**2d** only	30
5	DMAP only	14
6	**2a**/DMAP	583
7	**2a**/Py	301
8	**2a**/TEA	396
9	**2a**/TPA	237
10	**2a**/TBA	186
11	**2a**/MeIm	263
12	**2a**/DBU	465
13	**2a**/NMP	113
14	**2b**/DMAP	662
15	**2c**/DMAP	607
16	**2d**/DMAP	488

Reaction conditions: Catalyst (2.14×10^{-5} mol), propylene oxide (3 mL, 42.9 mmol, 2000 eq.), co-catalyst (4.3×10^{-5} mol), at 130 °C, for 3 hours, using 300 psig CO_2 pressure. DMAP – 4-dimethylamino pyridine; Py – pyridine; TEA – triethylamine; TPA – tripropylamine; TBA – tributylamine; MeIm – methylimidazole; DBU – 1,8-diazabicycloundec-7-ene; NMP – *N*-methyl-2-pyrrolidone. [a] Moles of propylene carbonate produced per mole of catalyst per hour.

absence of a co-catalyst. Significantly low TOFs were observed for propylene carbonate production, indicating that the system needs an active co-catalyst for better product yields. For this study, we studied a range of Lewis bases as co-catalysts along with complex **2** (Scheme 1). Table 3 shows the effect of various co-catalysts on the TOF of propylene carbonate production. From Table 3, the **2a**/DMAP (entry 6, Table 3) system gave a very high TOF of 583 h^{-1} for propylene carbonate formation in comparison with other bases; a low TOF of 113 h^{-1} was observed with the **2a**/*N*-methyl pyrrolidine system. From Table 3, diminishing activity was observed with less Lewis basic and bulky co-catalysts.

With DMAP found to be the choice co-catalyst, a further study on the influence of changes in its concentration indicated a profound effect on the TOF of the propylene carbonate formed. Fig. 5 reveals a change in TOF of propylene carbonate with a change in the concentration of DMAP with respect to the concentration of the catalyst. The TOF of propylene carbonate reaches its maximum when the ratio of **2a** : DMAP reaches 1 : 2. Beyond this catalyst to DMAP ratio, further increase in the concentration of the co-catalyst resulted in a decrease in the TOF, which may be due to excess DMAP saturating the catalyst binding positions, thus leaving no room for the binding of epoxide to the catalyst for further activity.

Once DMAP was found to be an active co-catalyst for the propylene carbonate formation, we have also studied the activity of other cobalt complexes. It is evident from Table 3 that all these cobalt complexes (**2a**–**2d**) were found to be active in producing propylene carbonate with a good TOF. TOFs of 662, 607, and 488 h^{-1} were observed for cobalt complexes with chlorine (**2b**), nitro (**2c**) and methyl (**2d**) groups in the ligand framework, respectively. The cobalt complex with electron withdrawing atoms such as chloro (**2b**) and nitro (**2c**) on the aromatic ring showed exceptionally high catalytic activity (entries 14 and 15, Table 3). Complexes **2a** and **2d** showed relatively lower activity, with the latter being the least active (entry 16, Table 3). This change in activity could be attributed to the change in Lewis acidity of the complexes.

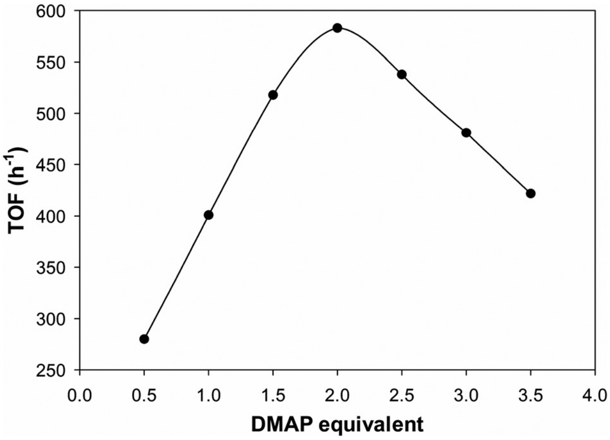

Fig. 5 Turnover frequency of the catalyst on propylene carbonate production using the catalyst **2a**/DMAP system as a function of DMAP equivalents. Reaction conditions: catalyst (2.14×10^{-5} mol), propylene oxide (3 mL, 42.9 mmol), 130 °C, CO_2 (300 psig) in 3 hours.

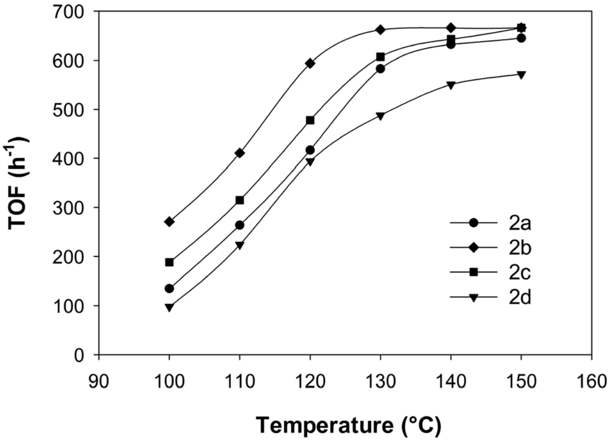

Fig. 6 Turnover frequency of the catalyst on propylene carbonate production for the catalyst **2a–d**/DMAP systems as a function of reaction temperature. Reaction conditions: catalyst (2.14×10^{-5} mol), propylene oxide (3 mL, 42.9 mmol, 2000 eq.), co-catalyst (DMAP, 4.3×10^{-5} mol), CO_2 pressure (300 psig) for 3 hours.

The activity of the cobalt complexes with DMAP was studied at different temperatures for the synthesis of propylene carbonate. Fig. 6 shows the TOF of propylene carbonate production at various temperatures. The product TOF increases with an increase in temperature; at 150 °C it was found to have completely converted to the product, indicating that complexes **2a**–**2d** were found to be stable at high reaction temperatures. In order to compare with other cobalt complexes, we chose 130 °C as the reaction temperature for the rest of the studies.

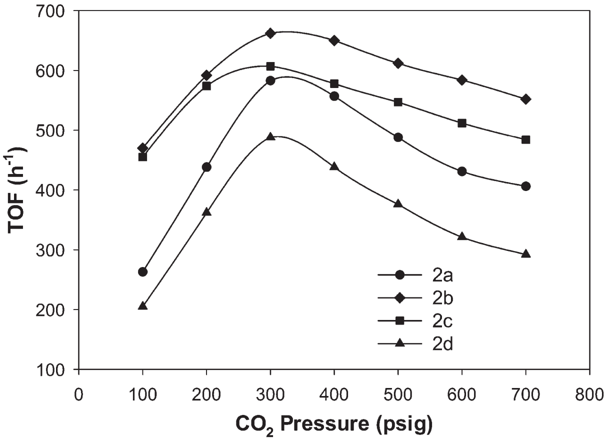

Fig. 7 Turnover frequency of the catalyst on propylene carbonate production for the catalyst **2a–d**/DMAP systems as a function of carbon dioxide pressure. Reaction conditions: catalyst (2.14 × 10^{-5} mol), propylene oxide (3 mL, 42.9 mmol, 2000 eq.), co-catalyst (DMAP, 4.3 × 10^{-5} mol), at 130 °C, for 3 hours.

Table 4 Study of the activity of the catalyst **2b** on various epoxides

Entry	Epoxide	Selectivity (%)	Yield (%)
1	Propylene oxide	99	~99
2	Epichlorohydrin	99	~99
3	Epoxydodecane	99	~92
4	Styrene oxide	94	71
5	Cyclohexene oxide	99	96[a]
6	Cyclooctene oxide	90	83[a]

Reaction conditions: catalyst (2.14 × 10^{-5} mol), substrate (21.5 mmol, 1000 eq.), co-catalyst (DMAP, 4.3 × 10^{-5} mol), at 130 °C, for 5 hours, using 300 psig CO_2 pressure. [a] Reactions were performed at 150 °C.

As the complex **2a**/DMAP was found to be an active catalyst system for the cycloaddition of carbon dioxide to epoxide, we determined the optimum CO_2 pressure for the reaction. The effect of carbon dioxide pressure was studied at 130 °C by employing a catalyst, a co-catalyst, and propylene oxide, while maintaining the ratio of 1 : 2 : 2000. Fig. 7 shows the influence of carbon dioxide pressure on the reaction of propylene oxide and CO_2. The maximum product yield was observed at 300 psig CO_2 pressure. This CO_2 pressure has been found to be optimum and similar to our previous work.[54] Similarly, other cobalt complexes (complexes **2b**, **2c** and **2d**) were also studied at various CO_2 pressures. The formation of product at 100 psig CO_2 pressure indicates that all these cobalt complexes were found to be active even at low reaction pressure. A similar trend of reactivity has been observed in our previous findings for CO_2/epoxide reactions catalyzed by cyclic metal amido complexes.[27,28]

The activity of the **2b**/DMAP system on the synthesis of cyclic carbonates using various aromatic and aliphatic epoxides was studied by employing the above optimized reaction conditions (300 psig, 130 °C in 3 h). Table 4 summarizes the yield of the various cyclic carbonates production. It is evident from this table that **2b**/DMAP is an efficient catalytic system on various aromatic and aliphatic epoxides for cyclic carbonate production.

2.3 Effect of substituents on reactivity

We also observed an increasing TON of propylene carbonate production over time with all four complexes (**2a**–**2d**). The maximum product TON was observed in 5 h with complex **2b**, which is the most active in the series. Fig. 8 shows the TON of propylene carbonate production at various time intervals. Considering the above results and previously reported metal catalyzed reaction mechanisms, we explained the effect of substituents on catalytic activity in the following way. The Lewis acid with the Lewis base initiated epoxide to cyclic carbonate reaction pathway has widely been discussed in many previous reports.[29,31] Initially, epoxide coordinated with the electrophilic metal center, and ring opening occurred with the aid of a nucleophile by forming an alkoxide intermediate. Insertion of CO_2 takes place, thus resulting in the formation of product by intramolecular cyclic elimination. Thus, the Lewis acidity of the Co(III) complex and nucleophilicity of the co-catalyst can influence the reaction mechanism. The presence of electron withdrawing groups, which increase the Lewis acidity of the metal center, directly affects the coordination of the epoxide; *i.e.*, epoxide coordination is easier with a strong acidic metal center.[29] As we observed in the above results, complex **2b** was found to be highly active in propylene carbonate production with TOFs of 662 h^{-1} whereas complex **2d** was found to be least active in the series with TOFs of 488 h^{-1}. The high catalytic activity of complex **2b** was attributed to the presence of two electron withdrawing chlorine groups, which make the metal center more electrophilic, and the low catalytic activity in the case of complex **2d** is due to the presence of two electron donating methyl groups. The catalytic activity order of cobalt complexes was observed as **2b** > **2c** > **2a** > **2d**. The activities of these cobalt complexes were evaluated over a period of time and increased activity was observed with increasing reaction

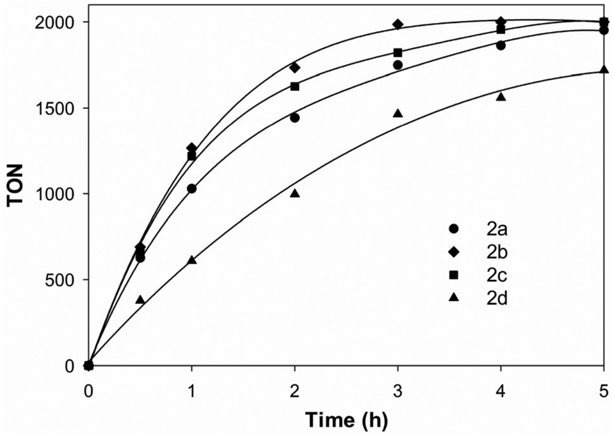

Fig. 8 Turnover number of the catalyst on propylene carbonate production for the catalyst **2a–d**/DMAP systems as a function of reaction time. Reaction conditions: catalyst (2.14 × 10^{-5} mol), propylene oxide (3 mL, 42.9 mmol, 2000 eq.), co-catalyst (DMAP, 4.03 × 10^{-5} mol), CO_2 pressure (300 psig) at 130 °C.

time. The high catalytic activity of complex **2b** was observed in all cases while studying the effect of CO_2 pressure, temperature, and reaction time. We have plotted TOF values of different catalysts against the Hammett parameters (σ_m) of various substituents on the complexes, which is shown in Fig. S23.† A linear relationship was observed between TOF and σ_m values of the substituents of the catalysts in the Hammett plot. The linear relationship supports our hypothesis on the effect of electron withdrawing and donating properties of various substituents of the ligand and how they affect Lewis acidity of metal complexes and, inevitably, the reactivity of the complexes.

3. Experimental

3.1 General

All chemicals used in this study were purchased from Aldrich Chemical Company, USA and Acros Chemical Company, USA and used without further purification unless otherwise mentioned. CO_2 (99.9%) was obtained from Airgas. All high pressure reactions were performed in a 100 mL Parr reactor connected with a 4840 controller. Tetrahydrofuran (THF) was dried over sodium and benzophenone. Elemental analyses were performed by Midwest Microlab Inc., Indianapolis.

3.2 Spectroscopy

^1H and ^{13}C-NMR spectra were obtained either using a 600 MHz Brüker instrument or a 400 MHz JEOL ECS 400 instrument equipped with a 5 mm triple resonance inverse probe. The spectra were collected at 25 °C, and chemical shifts were reported in ppm relative to TMS as the external standard, unless otherwise stated. Infrared spectra were obtained using a Thermo Scientific Nicolet 6700 FT-IR spectrometer. Electrospray ionization mass spectra (ESI-MS) were obtained using an Agilent 1000 series MSD VL spectrometer. Gas Chromatography Mass spectrometric (GC/MS) analysis was performed using an Agilent Technologies 6890N Network GC system and equipped with an Agilent Technologies 5975 inert XL mass selective detector.

3.3 Synthesis of amidoamine ligands (1) and their Co(III)-complexes (2)

All the amidoamine ligands (**1**) considered for this study were synthesized according to the previously reported procedure.[27,44] Ligands were characterized by ^1H and ^{13}C NMR studies (see ESI† for details).

Synthesis of the cobalt(III) complexes (**2**) was performed according to this general method. Ligand **1** (1 eq.) was dissolved in dry THF under N_2 and *n*-BuLi (2.1 eq., 1.6 M in hexane) was added at 0 °C. Dry solid $CoCl_2$ or $CoBr_2$ (1 eq.) was added to the solution. The solution was warmed up to room temperature and stirred overnight to yield a green precipitate. Air was admitted and a purple precipitate was collected. The mixture was filtered through silica gel, and the purple compound was eluted with methanol. The solution was evaporated to dryness under reduced pressure, and the resulting solid was washed with a small amount of dichloromethane yielding the product **2** as a purple powder.

Complex **2a**: Yield: 88%. Elemental analysis for $C_{14}H_{20}BrCoN_4O_2$: C, 40.50; H, 4.86; N, 13.49. Found: C, 40.36; H, 5.02; N, 13.54%. ESI-MS ($M - Br^+$): *m*/*z* 335.6 (Fig. S9†). ^1H NMR (CD_3OD, 3.33): 8.87 (m, 2H), 7.03 (m, 2H), 2.06 (s, 3H, CH_3CN), 1.611 (s, 12H). IR 1165 (aromatic amide), 1543 (aromatic), 1593 (carbonyl) and 3205, 3296 cm^{-1} (amine).

Complex **2b**: Yield: 90%. Elemental analysis for $C_{14}H_{18}BrCl_2CoN_4O_2$: C, 34.74; H, 3.75; N, 11.57. Found: C, 34.63; H, 3.84; N, 12.05. ESI-MS ($M - Br^+$): *m*/*z* 403 (Fig. S9†). ^1H NMR (CD_3OD, 3.33): 8.979 (s, 2H), 2.06 (s, 3H, CH_3CN), 1.585 (s, 12H). IR 678 (C–Cl), 1105 (aromatic amide), 1537 (Ph ring), 1596 (carbonyl) and 3232, 3320 cm^{-1} (amine).

Complex **2c**: Yield: 72%. Elemental analysis for $C_{14}H_{19}BrCoN_5O_4$: C, 36.54; H, 4.16; N, 15.22. Found: C, 36.46; H, 4.28; N, 15.35. ESI-MS ($M - Br^+$): *m*/*z* 380 (Fig. S9†). IR 1155 (aromatic amide), 1308 (nitro), 1537 (aromatic), 1596 (carbonyl) and 3203, 3284 cm^{-1} (amine).

Complex **2d**: Yield: 80%. Elemental analysis for $C_{16}H_{24}BrCoN_4O_2$: C, 43.36; H, 5.46; N, 12.64. Found: C, 43.48; H, 5.40; N, 12.54. ESI-MS ($M - Br^+$): *m*/*z* 362.1 (Fig. S9†). ^1H NMR (CD_3OD, 3.33): 8.639 (s, 2H), 2.304 (s, 6H), 2.06 (s, 3H, CH_3CN), 1.611 (s, 12H). IR 1234 (aromatic amide), 1521 (nitro), 1597 (carbonyl) and 3215, 3369 cm^{-1} (amine).

3.4 X-ray analysis

Suitable single crystals of the cobalt(III) complexes **2a** and **2b** were positioned in a MitiGen cryo-loop on the goniometer head of the Bruker APEX 2 diffractometer equipped with a SMART CCD area detector. Data sets were measured at 120 K. The intensity data were collected in ω scan mode using the Mo tube (Kα radiation; $\lambda = 0.71073$ Å) with a highly oriented graphite monochromator. Intensities were integrated from 4 series of 364 exposures, each covering 0.5° in ω at 20 seconds of acquisition time, with the total data set being a sphere.[55] The space group determination was done with the aid of XPREP software.[56,57] Numerical absorption corrections were applied based on crystal face indexing obtained using actual images recorded by the video-microscope camera (Fig. S10, S11, ESI†). Thus, absorption correction was performed using the SADABS program that was included in the Bruker AXS software package.[58] Both structures were solved by direct methods and refined by least squares on weighted F^2 values for all reflections using the SHELXTL program.[56] The final analysis of the variance between observed and calculated structure factors showed no apparent errors. The crystal data for compounds **2a** and **2b** are presented in Table 1, while bond lengths and valence angles are summarized in Table 2. Figures for the crystal structures of studied complexes were drawn using Mercury 4.1.2 and ORTEP 32 software[59,60] at a 50% thermal ellipsoids probability level. The PLATON checks of crystallographic data and actual CIF files for the reported structures can be found in the ESI.† CCDC numbers: 936734 (**2a**) and 936336 (**2b**).

3.5 Synthesis of cyclic carbonates

Scheme 1 illustrates the general method of synthesizing cyclic carbonates using epoxide and CO_2. A representative procedure for the coupling reaction of epoxides and CO_2 is as follows: a 100 mL stainless steel Parr high pressure autoclave was initially charged with a catalyst, DMAP and propylene oxide in the ratio 1 : 2 : 2000, respectively. The reaction vessel was initially pressurized with CO_2 and the system was allowed to equilibrate for about 2 min. Then the autoclave was heated to 130 °C and the reaction mixture was allowed to stir for 3 h under this condition. The vessel was then cooled quickly by placing in an ice/water bath and the pressure was released slowly. The reaction mass was collected in dichloromethane for complete transfer and the catalyst was separated by passing through a small plug of silica gel (2 g, 60–100 mesh) and eluting with dichloromethane. The solvent and the unreacted substrate were removed at reduced pressure. The yield was calculated either by taking the weight of the isolated product or by comparing the ratio of the product to substrate peak areas obtained by GC-MS analysis. Product yields were reported in TON (moles of the product formed per mole of catalyst) and TOF (moles of product formed per mole of catalyst in one hour). The product was characterized by IR, ^{1}H-NMR and GC-MS. All the experiments were run in duplicate.

4. Conclusion

In conclusion, we have synthesized a new class of cobalt complexes bearing various substituents and characterized them successfully. Structures of the complexes are identified by various spectroscopic techniques including X-ray crystallography studies. X-ray crystallography studies of these complexes indicate that the cobalt(III) complexes exist in six coordinated species in a solid form. Interestingly, due to the presence of Li^+, complex **2a** forms a chiral coordination polymer whereas complex **2b** is a neutral achiral complex. **2a** is particularly interesting as the ligand moiety is achiral, while during crystal formation it crystallizes into a chiral coordination polymer. All the cobalt(III) complexes are air stable, easily synthesized and found to be active in producing cyclic carbonates without any co-solvent. The activity of the complexes was examined on the production of propylene carbonate under various reaction conditions. Cyclic carbonates from various aliphatic and aromatic epoxides were synthesized effectively using cobalt(III) amidoamine complexes. Improved catalytic activity was observed with high Lewis acidic metal complex bearing electron withdrawing groups. Presence of both cobalt(III) catalyst and DMAP in a 1 : 2 molar ratio is necessary to obtain high catalytic activity.

The catalysts used in this process are strongly Lewis acidic enabling easy ring opening of epoxide substrates for CO_2 incorporation. The ability to alter the Lewis acidity by changing the substituent groups on the ligand provides a new system of catalysts whose activity can be further explored. The activity of the catalysts (TON ~1980) under relatively mild reaction conditions in the absence of a co-solvent, while maintaining the selectivity towards a single product (cyclic carbonate), is noteworthy. The possibility of the amidoamine ligand system to stabilize even the high-valent metal centers, availability of detailed crystal data, and the option of altering the activity of the catalyst by changing the substituent groups provide us with various opportunities to further explore the activity of these catalysts, especially in utilization of CO_2 for synthesizing value added products.

Acknowledgements

A.G. would like to thank the National Science Foundation EPSCoR program (grant EPS-1003970) for financial support and the National Science Foundation (grant CHE-1229149) major research instrument grant to complete this work. N.G. is grateful to Dr Nadia Marino (Syracuse University, SUNY) for her help with the resolution of complicated solvent molecules disorder in the crystal structure of **2a**.

References

1 D. H. Gibson, *Chem. Rev.*, 1996, **96**, 2063–2096.
2 C. Bolm, O. Beckmann and O. A. G. Dabard, *Angew. Chem., Int. Ed.*, 1999, **38**, 907–909.
3 I. Omae, *Catal. Today*, 2006, **115**, 33–52.
4 H. Arakawa, M. Aresta, J. N. Armor, M. A. Barteau, E. J. Beckman, A. T. Bell, J. E. Bercaw, C. Creutz, E. Dinjus, D. A. Dixon, K. Domen, D. L. DuBois, J. Eckert, E. Fujita, D. H. Gibson, W. A. Goddard, D. W. Goodman, J. Keller, G. J. Kubas, H. H. Kung, J. E. Lyons, L. E. Manzer, T. J. Marks, K. Morokuma, K. M. Nicholas, R. Periana, L. Que, J. Rostrup-Nielson, W. M. H. Sachtler, L. D. Schmidt, A. Sen, G. A. Somorjai, P. C. Stair, B. R. Stults and W. Tumas, *Chem. Rev.*, 2001, **101**, 953–996.
5 M. Shi and Y.-M. Shen, *Curr. Org. Chem.*, 2003, **7**, 737–745.
6 X. Xiaoding and J. A. Moulijn, *Energy Fuels*, 1996, **10**, 305–325.
7 T. Sakakura, J.-C. Choi and H. Yasuda, *Chem. Rev.*, 2007, **107**, 2365–2387.
8 W. Coates Geoffrey and R. Moore David, *Angew. Chem., Int. Ed.*, 2004, **43**, 6618–6639.
9 K. Beyer, W. Bergfeld, W. Berndt, W. Carlton, D. Hoffmann, A. Schroeter and R. Shank, *J. Am. Coll. Toxicol.*, 1987, **6**, 23.
10 R. Papciak and V. Mallory, *Acute Toxic. Data*, 1990, **1**, 15.
11 C. Ursin, C. Hansen, J. Van Dyk, P. Jensen, I. Christensen and J. Ebbehoej, *Skin. Am. Ind. Hyg. Assoc.*, 1995, **56**, 651.
12 M. Wakihara and O. Yamamoto, *Lithium Ion Batteries Fundamentals and Performance*, Kodansha Ltd, Tokyo, 1998.
13 J. Lucas and Z. Halar, *US Pat.*, 5,449,474, 1995.
14 J. Machac and T. Marquis, *U.S. Patent*, 6,187,108, 2001.
15 A. Shaikh and S. Sivaram, *Chem. Rev.*, 1996, **96**, 951.
16 T. Sakakura and K. Kohno, *Chem. Commun.*, 2009, 1312–1330.

17 A. Steblyanko, W. Choi, F. Sanda and T. Endo, *J. Polym. Sci., Part A: Polym. Chem.*, 2000, **38**, 2375–2380.

18 Y. Sun, J.-C. Liu, E. S. Kimbleton and J. C. T. Wang, *WO Pat.*, 1997-US16190, 9810742, 9810765, 1998.

19 J. F. Knifton and R. G. Duranleau, *J. Mol. Catal.*, 1991, **67**, 389–399.

20 A.-A. G. Shaikh and S. Sivaram, *Chem. Rev.*, 1996, **96**, 951–976.

21 J. Sun, S.-I. Fujita, F. Zhao and M. Arai, *Green Chem.*, 2004, **6**, 613–616.

22 Y. Zhao, C. Yao, G. Chen and Q. Yuan, *Green Chem.*, 2013, **15**, 446–452.

23 K. Yamaguchi, K. Ebitani, T. Yoshida, H. Yoshida and K. Kaneda, *J. Am. Chem. Soc.*, 1999, **121**, 4526–4527.

24 B. M. Bhanage, S.-I. Fujita, Y. Ikushima and M. Arai, *Appl. Catal., A*, 2001, **219**, 259–266.

25 P. Ramidi, P. Munshi, Y. Gartia, S. Pulla, A. S. Biris, A. Paul and A. Ghosh, *Chem. Phys. Lett.*, 2011, **512**, 273–277.

26 W. J. Peppel, *J. Ind. Eng. Chem.*, 1958, **50**, 767–770.

27 A. Ghosh, P. Ramidi, S. Pulla, S. Z. Sullivan, S. L. Collom, Y. Gartia, P. Munshi, A. S. Biris, B. C. Noll and B. C. Berry, *Catal. Lett.*, 2010, **137**, 1–7.

28 P. Ramidi, S. Z. Sullivan, Y. Gartia, P. Munshi, W. O. Griffin, J. A. Darsey, A. Biswas, A. U. Shaikh and A. Ghosh, *Ind. Eng. Chem. Res.*, 2011, **50**, 7800–7807.

29 K. B. Hansen, J. L. Leighton and E. N. Jacobsen, *J. Am. Chem. Soc.*, 1996, **118**, 10924–10925.

30 R. L. Paddock and S. T. Nguyen, *J. Am. Chem. Soc.*, 2001, **123**, 11498–11499.

31 R. L. Paddock and S. T. Nguyen, *Macromolecules*, 2005, **38**, 6251–6253.

32 X.-B. Lu and D. J. Darensbourg, *Chem. Soc. Rev.*, 2012, **41**, 1462–1484.

33 D. J. Darensbourg and R. M. Mackiewicz, *J. Am. Chem. Soc.*, 2005, **127**, 14026–14038.

34 M. North, P. Villuendas and C. Young, *Tetrahedron Lett.*, 2012, **53**, 2736–2740.

35 J. Liu, W.-M. Ren, Y. Liu and X.-B. Lu, *Macromolecules*, 2013, **46**, 1343–1349.

36 M. North and P. Villuendas, *ChemCatChem*, 2012, **4**, 789–794.

37 M. North and C. Young, *ChemSusChem*, 2011, **4**, 1685–1693.

38 J. Melendez, M. North, P. Villuendas and C. Young, *Dalton Trans.*, 2011, **40**, 3885–3902.

39 D. J. Darensbourg and M. W. Holtcamp, *Coord. Chem. Rev.*, 1996, **153**, 155–174.

40 J.-M. Pons and M. Santelli, *Lewis acids and selectivity in organic synthesis*, CRC Press, 1995.

41 M. North, R. Pasquale and C. Young, *Green Chem.*, 2010, **12**, 1514–1539.

42 S. Pulla, P. Ramidi, B. L. Jarvis, P. Munshi, W. O. Griffin, J. A. Darsey, J. L. Dallas, V. Pokala and A. Ghosh, *Greenhouse Gases Sci. Technol.*, 2012, **2**, 66–74.

43 S. Pulla, C. M. Felton, Y. Gartia, P. Ramidi and A. Ghosh, *ACS Sustainable Chem. Eng.*, 2013, **1**, 309–312.

44 S. Pulla, V. Unnikrishnan, P. Ramidi, S. Z. Sullivan, A. Ghosh, J. L. Dallas and P. Munshi, *J. Mol. Catal. A: Chem.*, 2011, **338**, 33–43.

45 S. T. Mak, W. T. Wong, V. W. W. Yam, T. F. Lai and C. M. Che, *J. Chem. Soc., Dalton Trans.*, 1991, 1915–1922.

46 M. Chopra, T. S. M. Hun, W.-H. Leung and N.-T. Yu, *Inorg. Chem.*, 1995, **34**, 5973–5978.

47 X. Xi, Y. Fang, T. Dong and Y. Cui, *Angew. Chem., Int. Ed.*, 2011, **50**, 1154–1158.

48 T. Liu, Y. Liu, W. Xuan and Y. Cui, *Angew. Chem., Int. Ed.*, 2010, **49**, 4121–4124.

49 Q. Yang, Z. Chen, J. Hu, Y. Hao, Y. Li, Q. Lu and H. Zheng, *Chem. Commun.*, 2013, **49**, 3585–3587.

50 J. Zhang, S. Chen, R. A. Nieto, T. Wu, P. Feng and X. Bu, *Angew. Chem., Int. Ed.*, 2010, **49**, 1267–1270, S1267/1261–S1267/1265.

51 W. M. Reichert, J. D. Holbrey, K. B. Vigour, T. D. Morgan, G. A. Broker and R. D. Rogers, *Chem. Commun.*, 2006, 4767–4779.

52 E.-Q. Gao, Y.-F. Yue, S.-Q. Bai, Z. He and C.-H. Yan, *J. Am. Chem. Soc.*, 2004, **126**, 1419–1429.

53 M. Calligaris, G. Nardin and L. Randaccio, *Coord. Chem. Rev.*, 1972, **7**, 385–403.

54 R. L. Paddock, Y. Hiyama, J. M. McKay and S. T. Nguyen, *Tetrahedron Lett.*, 2004, **45**, 2023–2026.

55 *SAINT, Data Integration Program*, Bruker AXS, Madison, WI, 1998.

56 R. H. Blessing, *Acta Crystallogr., Sect. A: Fundam. Crystallogr.*, 1995, **A51**, 33–38.

57 G. M. Sheldrick, *SADABS Area-detector Absorption Correction, 2.03*, University of Göttingen, Göttingen, Germany, 1999.

58 *Software Package for Crystal Structure Solution, APEX 2*, Bruker AXS, Madison, WI, 2009.

59 L. J. Farrugia, *J. Appl. Crystallogr.*, 1997, **30**, 565.

60 M. N. Burnett and C. K. Johnson, ORTEP III: Report ORNL-6895, Oak Ridge National Laboratory, Oak Ridge, TN, 1996.